

Supporting information

Endosomolytic and Tumor-Penetrating Mesoporous Silica Nanoparticles for siRNA/miRNA Combination Cancer Therapy

*Yazhe Wang,^{1, †, §} Ying Xie,^{1, †, §} Kameron V. Kilchrist,[‡] Jing Li,[†] Craig L. Duvall,[‡] David
Oupicky^{†*}*

[†] Center for Drug Delivery and Nanomedicine, Department of Pharmaceutical Sciences,
University of Nebraska Medical Center, Omaha, Nebraska, United States

[‡] Department of Biomedical Engineering, Vanderbilt University, Nashville, Tennessee, United
States

[§] Present address: Department of Biomedical Engineering, Yale University, New Haven,
Connecticut, United States

¹ These authors contributed equally

*Corresponding author: david.oupicky@unmc.edu

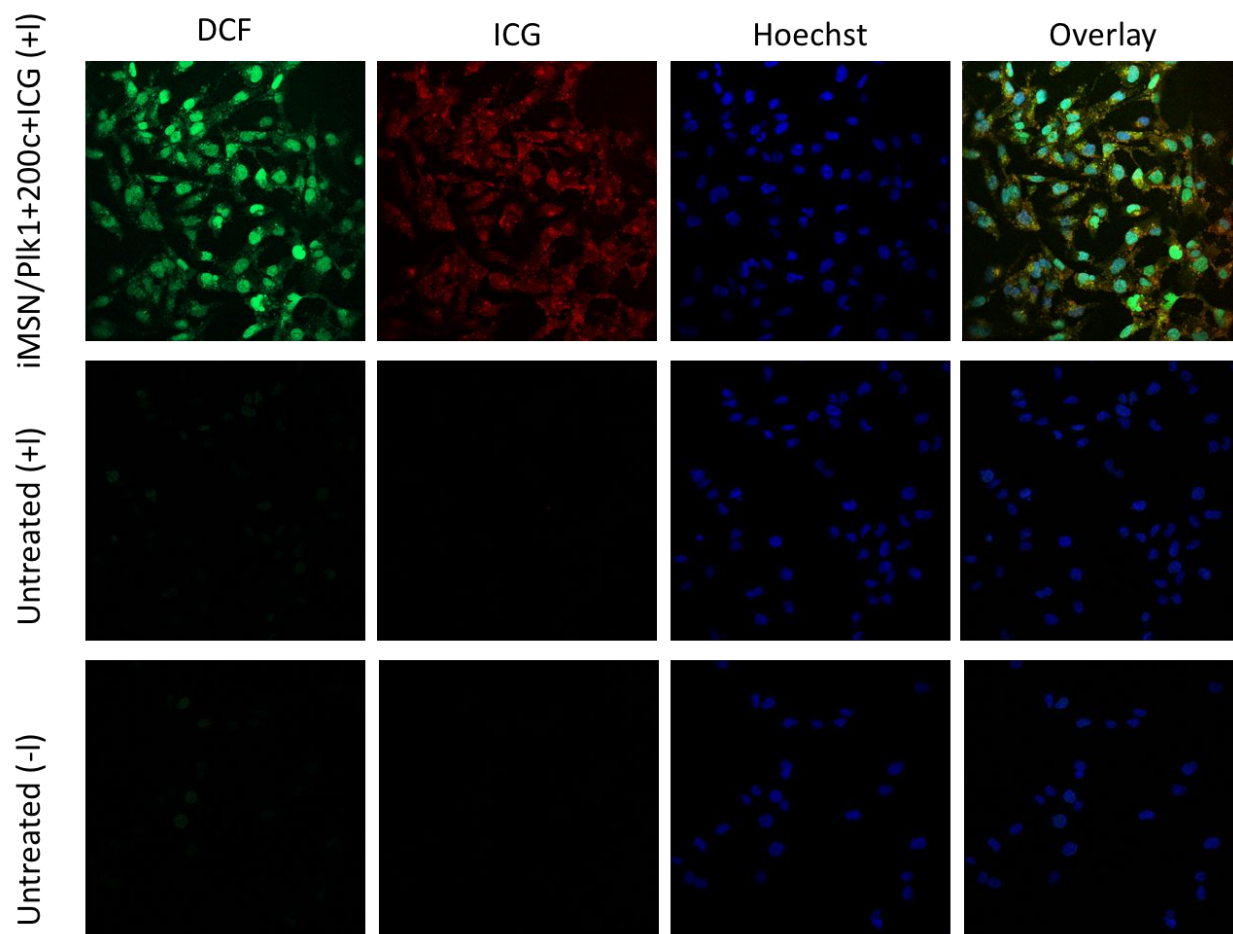


Figure S1. ROS generation following 4 h incubation of tumor cells with nanoparticle and laser irradiation. Confocal images of MDA-MB-231 cells stained by ROS detecting probe DCF (green). Cell nuclei were stained by Hoechst 33258.

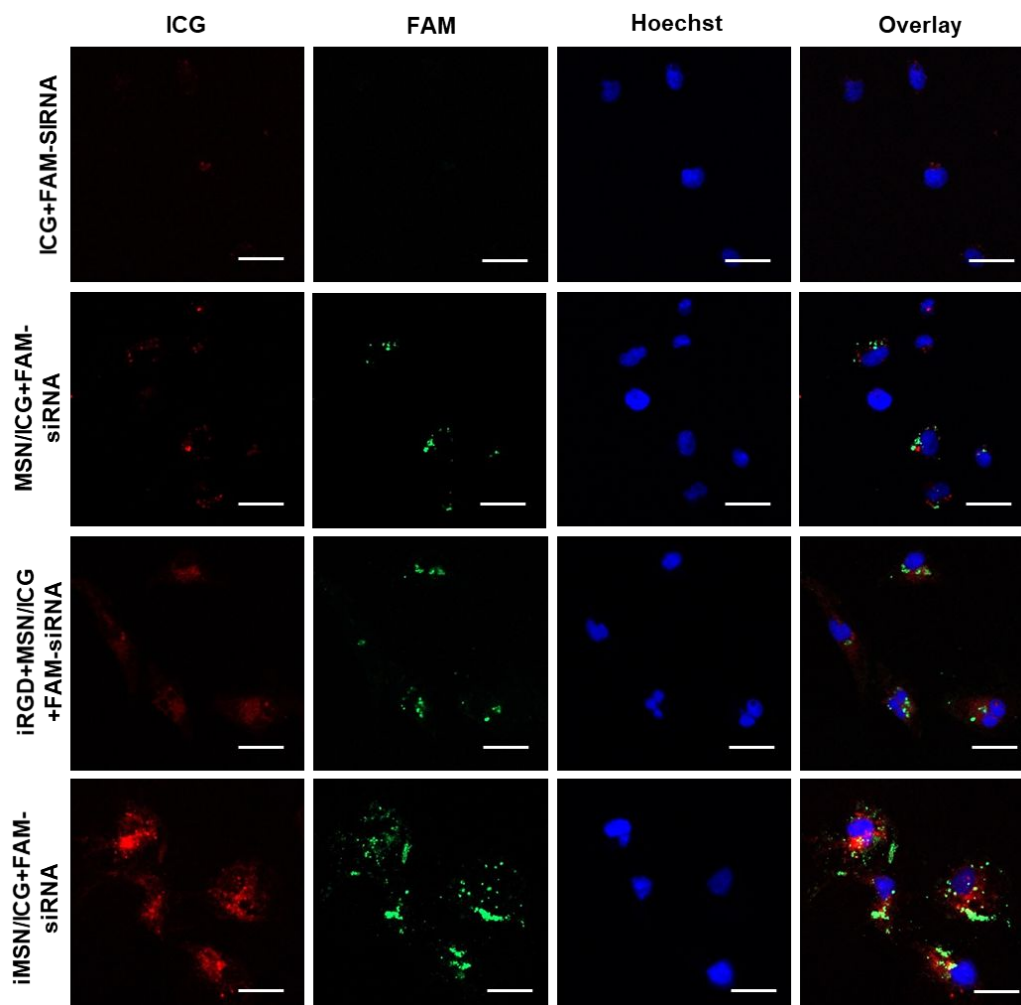


Figure S2. Cellular uptake in MDA-MB-231 cells by confocal microscopy. The cells were incubated with the nanoparticles or free ICG+FAM-siRNA for 4 h. Nuclei were stained with Hoechst dye. Red fluorescence of ICG, green fluorescence of FAM-siRNA. Scale bar, 20 μ m.

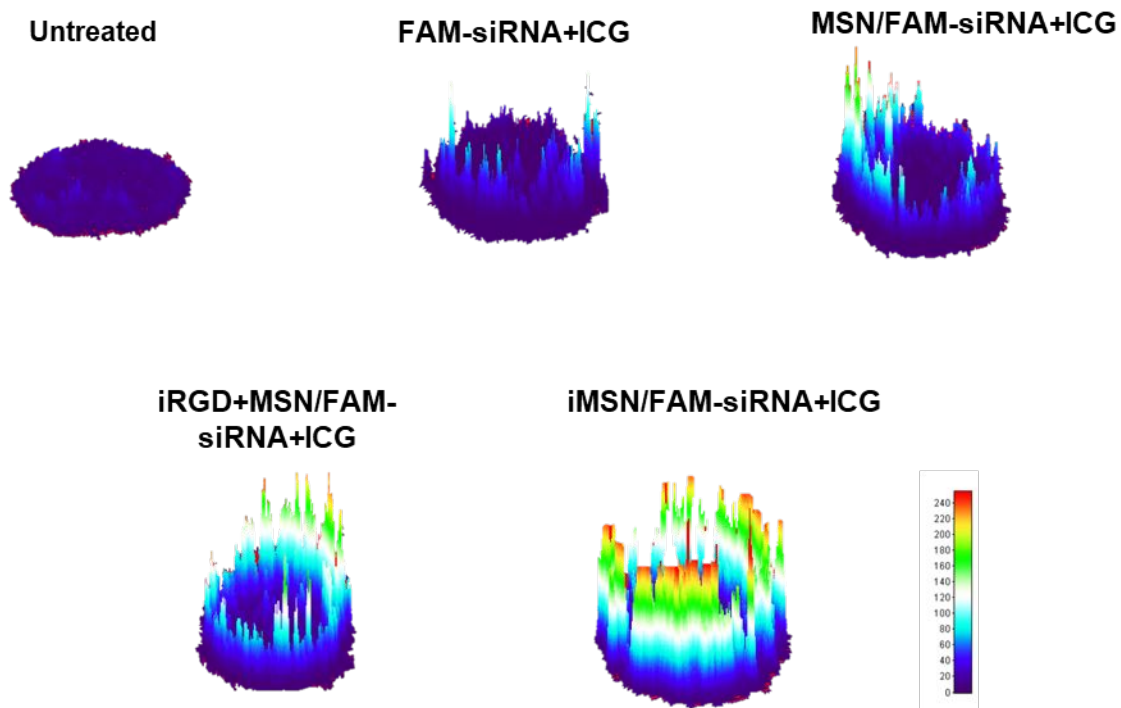


Figure S3. Surface plot images of MDA-MB-231 tumor spheroids treated with free FAM-siRNA+ICG, MSN/FAM-siRNA+ICG, iRGD+MSN/FAM-siRNA+ICG, iMSN/FAM-siRNA+ICG and negative control. Fluorescence signal was from FAM-siRNA channel.

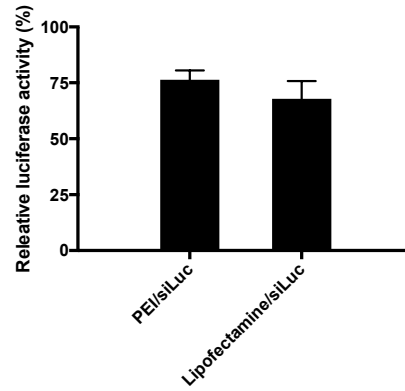


Figure S4. Luc silencing efficacy of siLuc loaded with PEI and Lipofectamine 3000 in MDA-MB-231.Luc cells. Data are shown as mean \pm SD (n = 3).

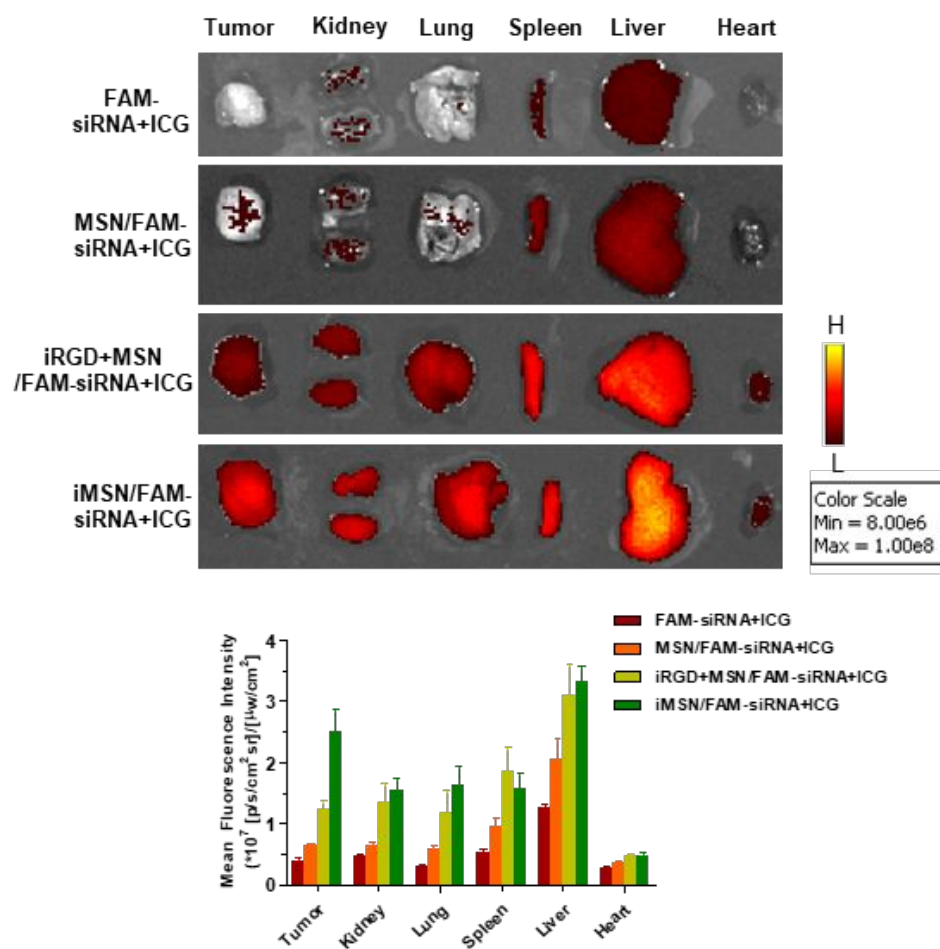


Figure S5. *Ex vivo* images of tumors and other tissues at 48 h after injection and semiquantification of nanoparticle biodistribution in mice tissues. Results are expressed as mean fluorescence intensity \pm SD (n = 3).

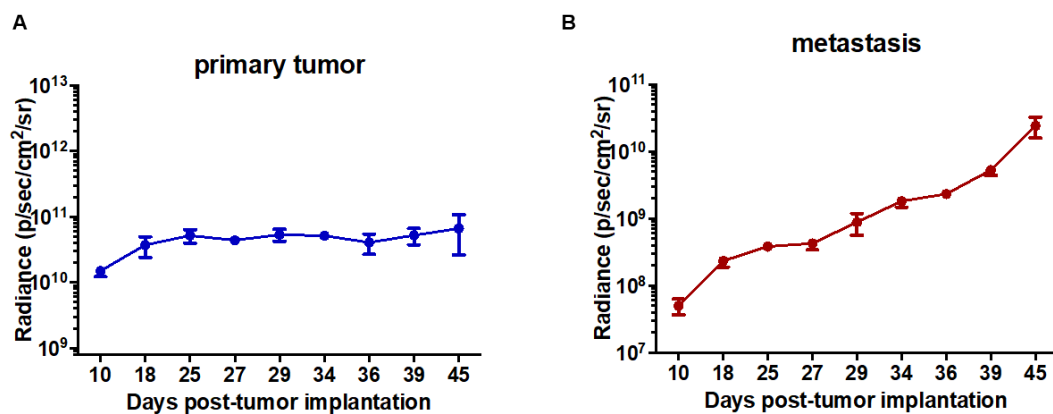


Figure S6. Quantitative analysis of bioluminescence signal from primary tumor (A) and metastasis (B) in untreated tumor-bearing mice post-tumor implantation. Results are expressed as mean fluorescence intensity \pm SD (n = 5).

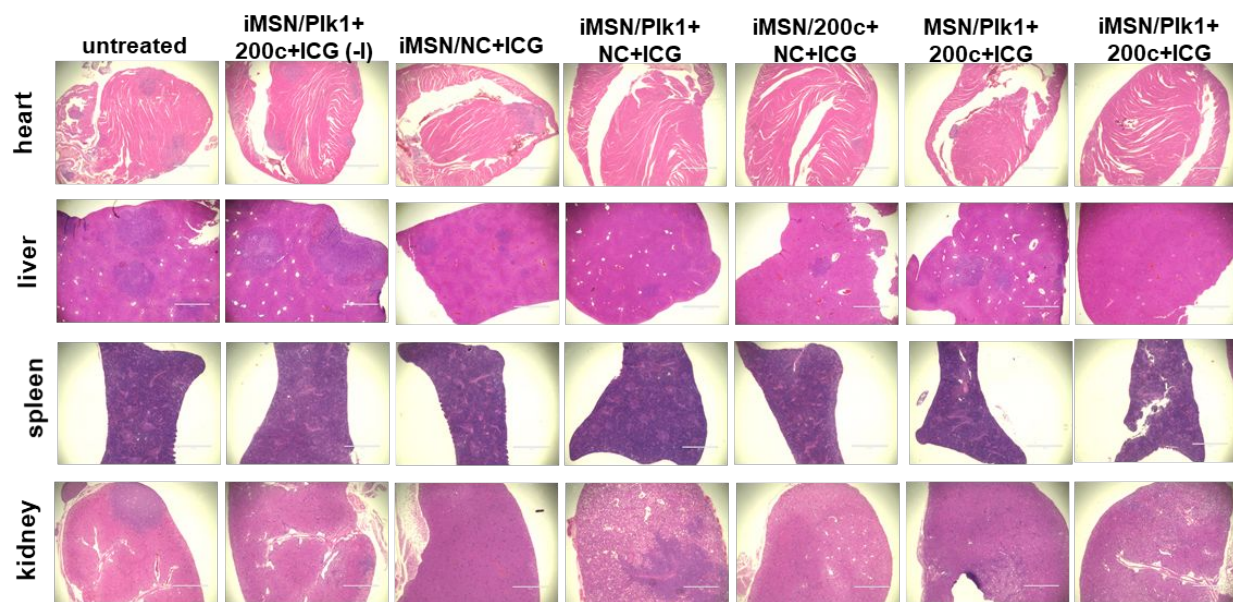


Figure S7. Histological observation of tissue sections from major organs of mice was performed after the treatment. The organ sections were stained with hematoxylin and eosin (H&E). Scale bar, 1000 μm (4x), 100 μm (40x).

Table S1. Blood biochemistry of tumor-bearing mice treated with iMSN/NC+ICG, iMSN/Plk1+200c+ICG (+/-light) or saline from the efficacy experiment.

	Saline	NC+ICG	Plk1+200c+ICG (-l)	Plk1+200c+ICG (+l)
WBC (10 ⁹ /L)	6.2±3.9	4.6±1.4	5.2±0.8	3.1±0.5
LYM (10 ⁹ /L)	0.7±0.6	0.6±0.3	0.5±0.2	0.9±0.6
MON (10 ⁹ /L)	0.4±0.2	0.4±0.1	0.4±0.1	0.2±0.2
NEU (10 ⁹ /L)	5.2±3.1	3.5±1.6	4.3±0.6	2.0±0.6
RBC (10 ¹² /L)	8.9±0.5	8.9±0.3	9.2±0.7	8.1±0.3
HGB (g/dL)	15.2±0.6	15.0±0.7	15.3±1.1	14.0±0.8
HCT (%)	42.1±3.7	40.7±1.5	41.7±2.9	35.9±1.5
MCV (fl)	46.0±0.0	46.0±0.0	46.0±1.0	45.0±0.0
MCH (pg)	16.7±1.0	16.8±0.3	16.7±0.1	17.6±0.5
MCHC (g/dL)	37.3±1.0	36.8±0.5	36.8±0.7	39.1±0.9
RDWc (%)	18.6±0.2	18.5±0.5	18.1±0.3	19.1±0.6
RDWs (fl)	34.1±0.5	34.1±0.9	32.8±0.8	34.4±0.8
PLT (10 ⁹ /L)	656±77	594±52	614±78	705±172
MPV (fl)	6.0±0.3	6.2±0.2	6.2±0.1	6.0±0.1
PCT (%)	0.4±0.1	0.4±0.0	0.4±0.1	0.4±0.1
PDWc (%)	29.3±0.6	29.3±0.6	30.5±1.0	29.1±1.2
PDWs (fl)	6.1±0.3	6.1±0.3	6.6±0.5	6.0±0.5
BUN (mg/dL)	26.2±2.5	24.2±4.5	28.0±7.3	20.7±7.1
CRE (mg/dL)	2.2±0.2	2.2±0.6	1.9±0.1	1.7±0.3
AST (U/L)	29.0±1.2	27.5±6.6	26.3±4.7	26.1±2.5
ALT (U/L)	4.5±0.9	5.1±1.5	5.3±1.0	5.3±0.6